SYNTHESIS AND CHARACTERIZATION OF AN ISOLEUCINE-CONTAINING MACROCYCLE

by

Camryn Gloor

Submitted in partial fulfillment of the
requirements for Departmental Honors in
the Department of Chemistry and Biochemistry
Texas Christian University
Fort Worth, Texas

May 2, 2022

SYNTHESIS AND CHARACTERIZATION OF AN ISOLEUCINE-CONTAINING MACROCYCLE

Project Approved:

Supervising Professor: Eric Simanek, Ph.D.

Department of Chemistry and Biochemistry

Kayla Green, Ph.D.

Department of Chemistry and Biochemistry

Mikaela Stewart, Ph.D.

Department of Biology

ABSTRACT

Large drugs—including macrocycles—are receiving more attention due to the belief that there may be therapeutic targets available to them that are unavailable to small molecules. Here, the synthesis of an isoleucine-containing macrocycle comprising 24 atoms utilizes a three-step synthesis with intermediates that can all be isolated, purified, and characterized. The choice of isoleucine reflects a desire to understand how a large, *beta*-branched amino acid affects synthesis and conformation. The monomer is available in two reactions. First, a sequential substitution of cyanuric chloride with BOC-protected hydrazine, isoleucine, and dimethylamine gives the carboxylic acid intermediate. The three reactions are performed in a single reaction vessel and are monitored by thin-layer chromatography to ensure that each substitution was successful. The carboxylic acid intermediate is purified using silica gel chromatography. Then, an EDC-mediated coupling reaction between the acetal and an aminoacetal gives the monomer. The monomer can be envisioned to be crescent-shaped. Spontaneous dimerization is initiated by treating the monomer with trifluoracetic acid. Oligomeric and polymeric materials are not observed in synthesis. NMR spectroscopy confirms the successful synthesis of each intermediate and the macrocycle. Both COSY and rOesy spectra are used to probe the change in conformation as a function of solvent. Finally, NMR spectra are measured at various temperatures to help understand the dynamic behavior of the macrocycle.

ACKNOWLEDGEMENTS

I would like to thank everyone that helped me make this honors thesis a possibility. Specifically, a huge thank you to Dr. Eric Simanek for guiding me through the highs and lows of this project – I could not have achieved this without you. Thank you to Drs. Kayla Green and Mikaela Stewart for serving on my committee and guiding me throughout the writing process. To the professors within the Department of Chemistry and Biochemistry, thank you for sharing your wisdom and helping me fall in love with chemistry a little more each day. Thank you to my friends and family for their endless support, love, and patience. It does not go unnoticed. Finally, thank you to the John V. Roach Honors College and the College of Science and Engineering for this opportunity and for making this project a possibility. Financially, this research was supported by the Texas Christian University grant for undergraduate research (SERC-UG-200707), the National Institutes of Health, and the Robert A. Welch Foundation.

TABLE OF CONTENTS

TERMINOLOGY AND ABBREVIATIONS

Abbreviation	Full Term
BOC	tert-butyloxycarbonyl
BRo5	beyond rule of 5
C	carbon
COSY	homonuclear correlation spectroscopy
DCM	dichloromethane
DIPEA	diisopropylethylamine
DMA	dimethylamine
DMSO	dimethylsulfoxide
H	hydrogen
MeOH	methanol
MeOD-d_4	deuterated methanol
NMR	nuclear magnetic resonance spectroscopy
PPI	protein-protein interactions
ppm	parts per million
Ro5	rule of 5
ROESY	rotating frame overhause effect spectroscopy
TLC	thin-layer chromatography
THF	tetrahydrofuran

FIGURES AND SCHEMES

INTRODUCTION

Within the last twenty years, macrocyclic drugs have become of interest due to their ability to target protein surfaces that were traditionally considered "undruggable."[1] Macrocycles can selectively recognize and effectively bind to these problematic targets because of their size and complexity.[2] The most prominent undruggable targets are the intracellular proteins involved in protein-protein interactions (PPIs).[3] PPIs do not have well-defined active sites marked with hydrophobic pockets for small molecule drugs to bind. Antibodies cannot cross the cell membrane to reach these targets.[3] In order for macrocycles to successfully target intracellular targets, cellular transport must be possible. This requirement presents a challenge as hydrophilicity is required for solubility in an aqueous solution, but hydrophobic properties are needed to cross the cellular membrane.[4]

Traditionally, drug design has been limited to small molecules that follow Lipinski's rule of five (Ro5). Lipinski's Ro5 gives a set of guidelines used for molecules when defining drug-like behavior and oral availability.[5] The Ro5 states that effective drugs should have: (1) no more than five hydrogen bond donors, (2) no more than ten hydrogen bond acceptors, (3) a molecular mass less than 500 Da, (4) partition coefficient not greater than five.[6] Large macrocycles like cyclosporin with many hydrogen bond donors and acceptors break Lipinski's rule. Today, there is a new focus on violators of the rule of 5 that venture into the "beyond the rules of 5" space (BRo5). Since approximately 6% of oral drugs are outside Lipinski's rules, it suggests there are areas to explore BRo5.[7]

The motivation for this research was to find an efficient way to synthesize macrocycles containing a beta-branched amino acid, isoleucine. The effective route involves the preparation of a monomer containing a triazine core with an auxiliary group, an amino acid, a hydrazine group, and an acetal group. The monomer, **I**, shown in Scheme 1, is available in two steps through an acid intermediate that can be isolated and purified. Upon the addition of an acid to **I,** two crescent-shaped monomers react and form the macrocycle, **I-I**. The macrocyclization to **I-I** is quantitative and does not require purification.

Scheme 1. Macrocycle **I-I** and the Monomer **I**

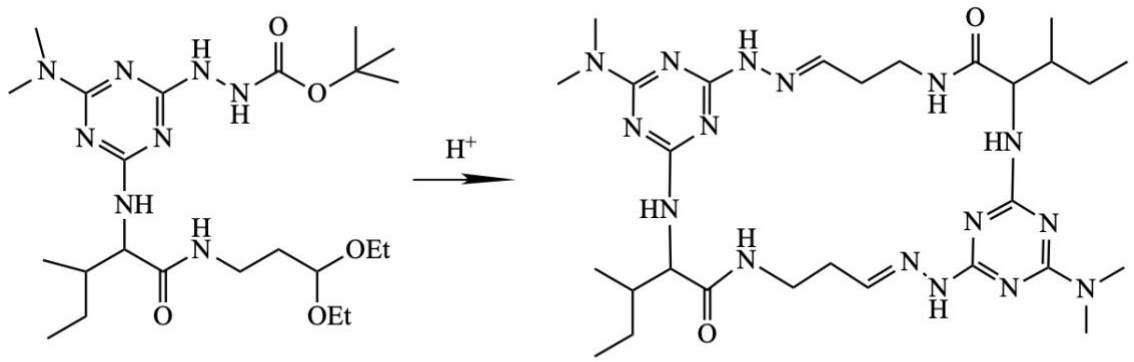

I **I-I**

Macrocycles also present a challenge because of their large number of rotatable bonds and conformational biases.[8] For macrocycles to be practical therapeutics, a "chameleon-like" character is required wherein the macrocycle can adopt various conformations. This flexibility allows macrocycles to present hydrophilic groups in an aqueous environment and reach a compact hydrophobic structure to facilitate cellular transport. It is thought that effective macrocyclic drugs will quickly move between extended and compact conformations.

Macrocycle **I-I** is novel because of the inclusion of isoleucine. Previous macrocycles synthesized included either glycine or *beta*-alanine.[9] Neither of these amino acids present sidechains that can offer better drug behavior at the cost of synthetic accessibility or conformational biases. Isoleucine is a *beta*-branched amino acid. We hypothesized that the branched sidechain of isoleucine would stabilize specific different conformations of the macrocycle.[10] These modifications to the amino acid can significantly affect shape by masking backbone amides. These changes should also greatly increase membrane permeability by increasing the hydrophobicity of the molecule.[11]

To examine these hypotheses, two-dimensional NMR spectroscopy was employed. Both COSY and rOesy spectra were obtained to establish the conformations that the macrocycle adopts based on solvent. Recording NMR spectra at various temperatures offers insight into the movement between the extended and folded conformations.

EXPERIMENTAL

NMR Spectroscopy. NMR spectra were recorded on a 400 MHz Bruker Avance spectrometer. Chemical shifts for ^{1}H and ^{13}C NMR spectra (in parts per million) were referenced to a corresponding residual solvent resonance. A rOesy spectrum was measured to note the impact of solvent on the structure. For rOesy experiments, the d1 delay was set at 2 sec, and d8 was set at 200μsec.

General Chemistry. Flash chromatography experiments were carried out on silica gel (Silicycle) with a porosity of 60Å, particle size of 50 – 63 μm, surface area of 500 – 600 m^2/g, a bulk density of 0.4 g/mL, and a pH range of 6.5 – 7.5. Dichloromethane/methanol was used as the eluent for chromatographic purification. Thin-layer chromatography experiments were visualized with UV

or submersion in ninhydrin (1.5g ninhydrin in 100mL of n-butanol and 3.0mL acetic acid) followed by heating. Excess solvents were removed using rotary evaporation on a Buchi Rotavapor RII with a Welch Self-Cleaning Dry Vacuum System. All workup and purification procedures were carried out with reagent-grade solvents under ambient atmosphere.

*Macrocycle **I-I**.* Monomer **I** (17.5 mg, 0.034 mmol) was dissolved in 1 mL of dichloromethane (DCM) in a 3 mL vial equipped with a stir bar. Trifluoroacetic acid (1 mL) was added dropwise to the reaction vial via pipette. The vial cap was not placed back on the vial, and the vial was left open. Evaporation occurred over the course of 7 days. The resulting residue was analyzed by NMR to establish purity. ^{1}H NMR (DMSO-*d*$_6$, 400 MHz): δ 12.6 (s, 1H), 11.4 (m, 1H), 9.20 (m, 1H), 7.48 (s, 1H), 7.19 (m, 1H), 4.30 (m, 2H), 3.10 (m, 6H), 2.99 (m, 1H), 2.62 (s, 1H), 1.77 (m, 1H), 1.57 (m, 1H), 1.24 (m, 2H), 0.99 (m, 3H), 0.91 (m, 3H). ^{13}C{^{1}H} NMR (DMSO-*d*$_6$, 100 MHz): δ 173.5, 161.9, 153.7, 148.4, 59.3, 59.6, 37.3, 36.5, 33.9, 31.8, 26.1, 25.3, 15.6, 15.2, 11.9, 11.3.

*Monomer **I**.* Intermediate **1** (180 mg, 0.47 mmol) was added rapidly as a solid to 1.1 mL of stirring DCM that was previously cooled to 0 ºC using an ice bath. This temperature was maintained while a solution of EDC-HCl (270 mg, 1.41 mmol) in 3.5 mL of DCM was added dropwise over a minute using a pipette. Once the addition was complete, 0.16 mL of diisopropylethylamine (119 mg, 0.92 mmol) was added dropwise over a minute yielding a colorless solution. After 30 minutes, thin-layer chromatography (10% methanol in DCM) confirmed the single spot starting material (R_f = 0.7) had disappeared, and a new spot at an R_f = 0.5 was observed under short wave UV irradiation. While maintaining the ice bath, a solution of diethoxypropylamine (96.7 mg, 1.64 mmol) in 1.6

mL DCM was added dropwise over 1 minute. The reaction was allowed to stir and warm to room temperature for four days. Thin-layer chromatography (TLC) suggested that all starting material had been consumed. The solution was extracted with three 50 mL portions of H_2O. The pale-yellow organic layer was dried using Mg_2SO_4, and the solvent was removed via rotary evaporation. The product was further purified using column chromatography (5% methanol in DCM) to yield 35 mg (23%) of pure material. ^{1}H NMR (DMSO- *d*$_6$, 400 MHz): δ 8.53 (m, 1H), 8.26 (m, 1H), 7.53 (m, 1H), 6.46 (m, 1H), 4.46 (m, 1H), 4.29 (m, 1H), 3.54 (m, 2H), 3.39 (m, 2H), 3.09 (m, 2H), 3.01 (s, 6H), 1.78 (s, 1H), 1.64 (m, 2H), 1.40 (s, 9H), 1.28 (m, 2H), 1.10 (m, 6H), 0.83 (m, 6H). ^{13}C{^{1}H} NMR (DMSO- *d*$_6$, 100 MHz): δ 167.8, 156.5, 100.9, 79.0, 61.3, 59.1, 36.9, 35.8, 35.1, 33.8, 28.6, 26.3, 25.3, 16.0, 15.8, 15.4, 12.2, 11.5.

*Intermediate **1.*** Cyanuric chloride (1.01 g, 5.49 mmol) was added rapidly as a solid to 28 mL of THF that was cooled to -10 ºC utilizing a dry ice and acetone bath. Dissolution of the solid occurs immediately. While maintaining a -10 ºC temperature, BOC-hydrazine (0.71 g, 5.44 mmol) was added dropwise at 2 drops per second using a pressure equilibrating addition funnel. Throughout the addition, the solution turned a rich yellow. Once the addition was complete, 1.10 mL of 5M NaOH (5.48 mmol) was added via pipette. After 1.5 h, thin-layer chromatography (10% methanol in dichloromethane) confirmed that a single product was observed under short wave UV irradiation (R_f = 0.7) or using ninhydrin (yellow spot). The dry ice bath was removed, and the solution was allowed to warm to room temperature. A solution of isoleucine (1.44 g, 10.97 mmol) in 11.0 mL of H_2O and 16.5 mL of 1M NaOH was added dropwise at a rate of 2 drops per second via a pressure equilibrating addition funnel. The solution immediately darkened to bronze, then lightened to a faint yellow throughout the reaction. The reaction mixture had a pH of 9 after the addition. After

24 h, 1 mL of 5M NaOH was added to maintain a pH of 9. After seven days, thin layer chromatography showed the starting material ($R_f = 0.7$) disappeared, and a new spot at $R_f = 0.05$ appeared. Then, dimethylamine (DMA, 1.24 g, 27.5 mmol) was added dropwise over three minutes (DMA was used as 40% aqueous solution). After 2 h, 1.2 mL of 1M HCl (1.2 mmol) was added dropwise via pipette until the pH = 9. The reaction was stirred for another 24 h at room temperature. Thin-layer chromatography showed the appearance of a new spot at $R_f = 0.25$. Brine was added to the reaction flask until a solid persisted. Then, the solution was extracted with three 80 mL portions of ethyl acetate. The organic layer was dried using $Mg_2SO_4$and the solvent was removed via rotary evaporation. Column chromatography was performed using 5% methanol in dichloromethane, yielding 243 mg pure product (8.6%). ^{1}H NMR (DMSO- *d*$_6$, 400 MHz): δ 12.4 (s, 1H), 8.57 (m, 1H), 8.17 (m, 1H), 6.59 (m, 1H), 4.37 (m, 1H), 3.35 (s, 2H), 3.01 (s, 6H), 1.85 (s, 1H), 1.40 (s, 9H), 1.30 (s, 2H), 0.88 (m, 6H). ^{13}C{1H} NMR (DMSO- *d*$_6$, 100 MHz): δ 174.5, 167.8, 166.3, 165.9, 156.5, 78.9, 58.5, 57.8, 57.3, 37.3, 36.6, 36.2, 35.7, 28.6, 25.3, 16.1, 11.9, 11.7, 11.6.

RESULTS AND DISCUSSION

Synthesis and Characterization of Monomer. The synthetic route for the monomer begins with cyanuric chloride, which undergoes three substitution reactions in solution to give an acid intermediate, **1**. The acid intermediate then undergoes an acetal coupling to give the monomer, **I** (**Scheme 2).** The order of substitution is due to the reactivity of the nucleophiles and the solubility of the intermediates.

Scheme 2. Synthesis of the monomer. a) $BOCNHNH_2$, NaOH *(aq)*, THF, -10 ºC, 1.5 h. b) Ile, NaOH (aq), RT, 1 wk. c) 40% $HN(CH_3)_2$ *(aq)*, RT, HCl *(aq)*, 24 h. d) EDC-HCl, DIPEA *(aq)*, 0 ºC, 30 min. e) diethoxypropylamine, RT, 4 d.

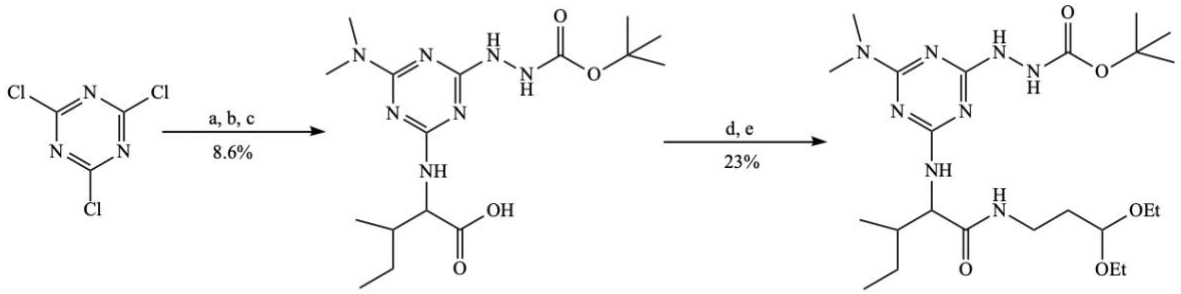

BOC-hydrazine is highly reactive and would react well as the third substitution. However, it was chosen for the first substitution because it is an easily handled solid. Secondly, the BOC group increases the solubility of the resulting dichlorotriazine and monochlorotriazine after adding isoleucine. The reaction is performed at -10 ºC to prevent double or triple substitution. The pH of the reaction is monitored to ensure that the BOC group is not cleaved.

Isoleucine was substituted second at room temperature. This again was done in the interest of solubility. The addition of isoleucine took longer than expected, probably due to the bulkiness of the amino acid. DMA is added last as a 40% aqueous solution that is readily used in excess.

All three reactions are completed in the same flask and monitored by thin-layer chromatography. The reactions proceed spot-to-spot. Isolation of the intermediate, **1**, is accomplished by extraction and yields 243 mg of pure product (8.6%). The low yield is expected to result from the pH being too low as optimization of the reaction conditions has led to increased yield.[12] The acid synthesis

was confirmed by ^{1}H and ^{13}C NMR obtained in DMSO-d_6. The labeling strategy used for assigning the NMR spectra is shown in **Chart 1.**

Chart 1. Labeling system of hydrogens and carbons in the NMR spectra.

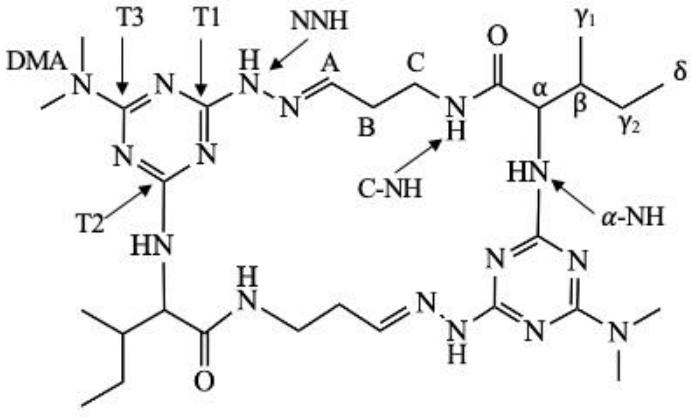

The same label is used for both the carbon and the protons attached whenever appropriate. The triazine carbons are identified as T1, T2, and T3. The order reflects the order of addition to the triazine nucleus. The dimethylamine groups are identified as DMA. The amino acid resonances are identified using Greek letters α-δ, such as H_α. The NH of the amino acid is identified as α−NH, while the carbonyl is CO. The hydrazine NH is identified as NNH. The acetal linker is identified using A-C with A corresponding to the most oxidized carbon. In the spectra of the monomer, the acetal is labeled as "acetal CH_3" or "acetal CH_2" when appropriate. Accordingly, the acetal NH is identified as C-NH. The proton that appears on the triazine ring when the ring is protonated is referred to as H^+. The labeling system employed when referring to specific resonances in the ^{1}H or ^{13}C spectra is shown in **Chart 1** and is conserved across all species.

The ^{1}H NMR spectrum of the intermediate **1** has identifying resonances from each substitution, including those correlating to BOC-hydrazine, isoleucine, and DMA (**Figure 1)**. The appearance of these resonances unambiguously proves that the synthesis was successful.

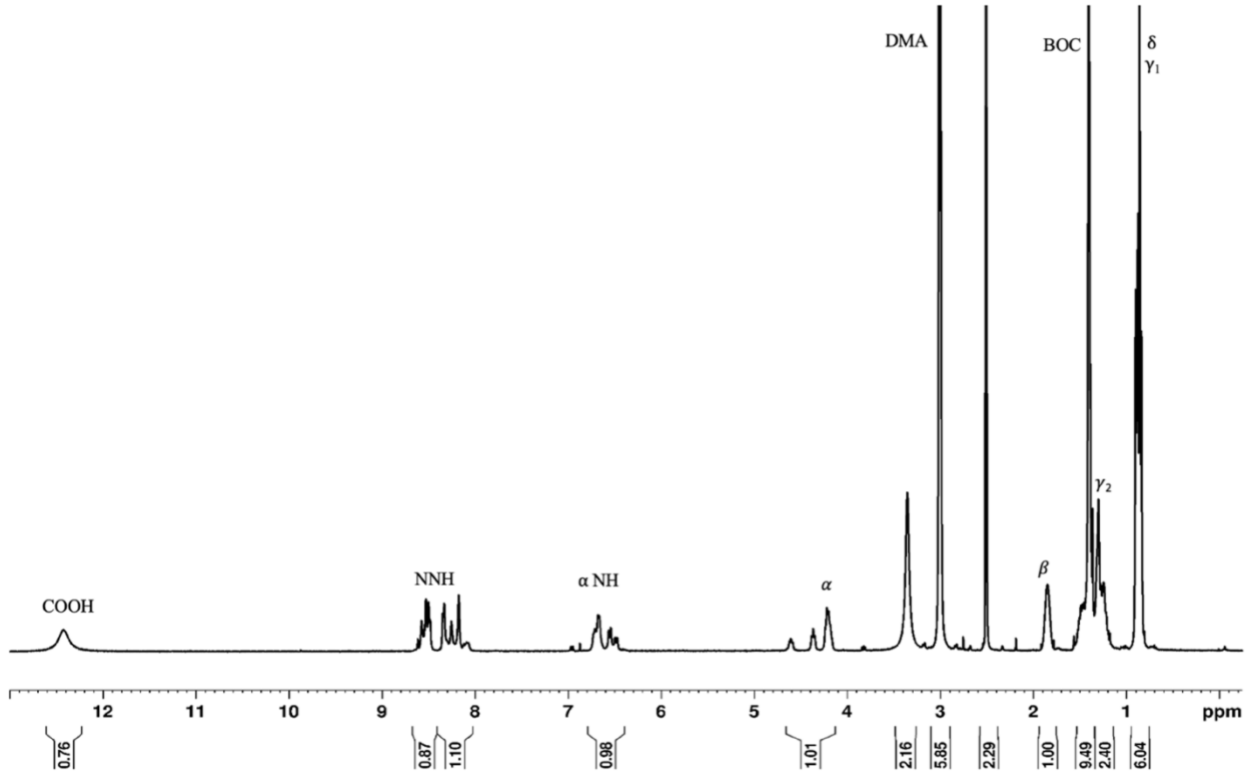

Figure 1. ^{1}H NMR spectrum of **1** in DMSO-d_6.

More specifically, the single peak appearing at 1.40 ppm is assigned to the BOC group. Similarly, multiple isoleucine peaks are identified including the terminal methyl groups at 0.88 ppm. A peak at 12.4 ppm indicates the presence of a carboxylic acid. Finally, the doublet at 3.01 ppm is representative of DMA.

Still, the ^{1}H NMR of **1** is not as simple as expected. For instance, while there is only one alpha-H of the amino acid, the spectrum shows three broad resonances for this proton. There is only one

α-NH in the structure, but the spectrum shows three broad resonances. There is only one NNH in the molecule, but the spectrum shows three broad resonances. The appearance of these multiple resonances is consistent with a molecule that adopts many slowly interconverting conformations in solution. This behavior is consistent with the literature and results from hindered rotation about the triazine-N bond.[13] Because the multitude of resonances points toward interconverting conformations, it is confirmed the acid intermediate was synthesized successfully and the product was not a mixture of components.

The ^{13}C NMR of **1** is shown in **Figure 2**. Similar to the ^{1}H spectra, single carbons sometimes give multiple resonances. In a ^{13}C NMR, electron-rich carbons shift upfield, while electron-poor carbons are found at higher ppms. It is possible to assign carbons in the spectra based on the environment in which they are found. A characteristic peak at 156 ppm shows three resonances for the triazine ring. Unreacted cyanuric chloride has symmetric carbons and presents a single peak at 172 ppm. The appearance of the triazine ring as three resonances upfield confirms the attachment of the substituents. A mass spectrum was measured to verify the synthesis of the intermediate (**Figure 3)**. The experimentally determined mass (M_{exp} = 384.2360 Da) matches the predicted mass (M_{pred} = 384.2354 Da) of the intermediate, **1.**

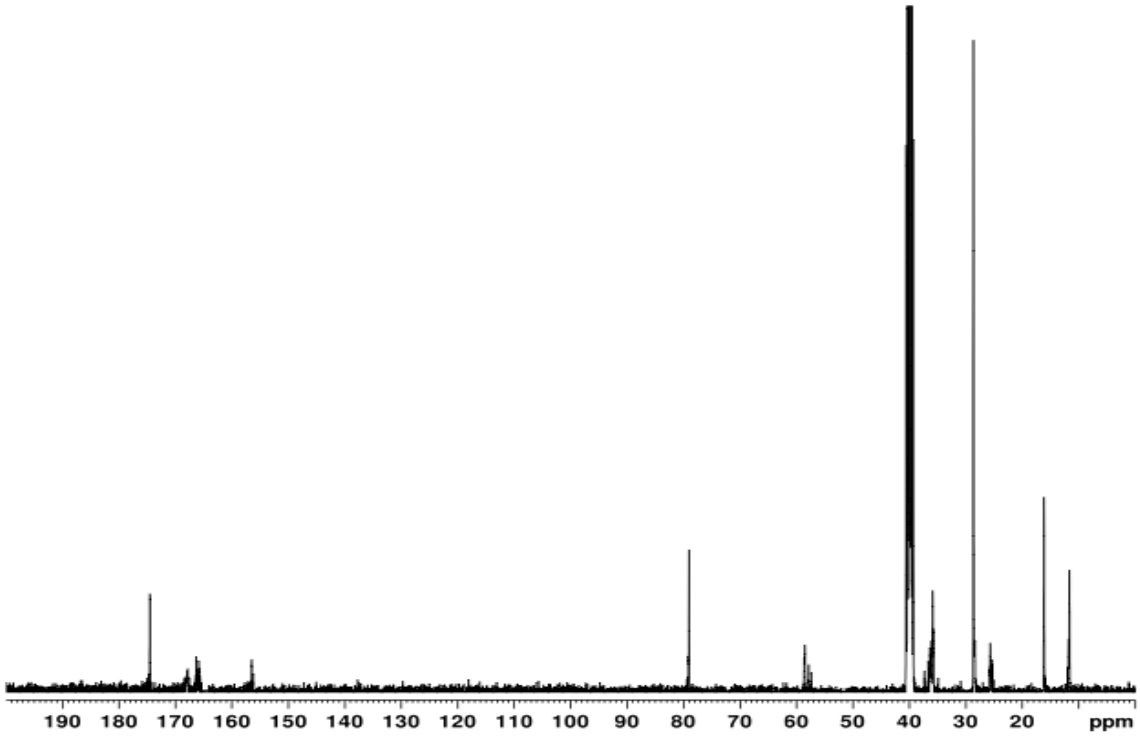

Figure 2. ^{13}C NMR spectrum of **1** in DMSO-d_6.

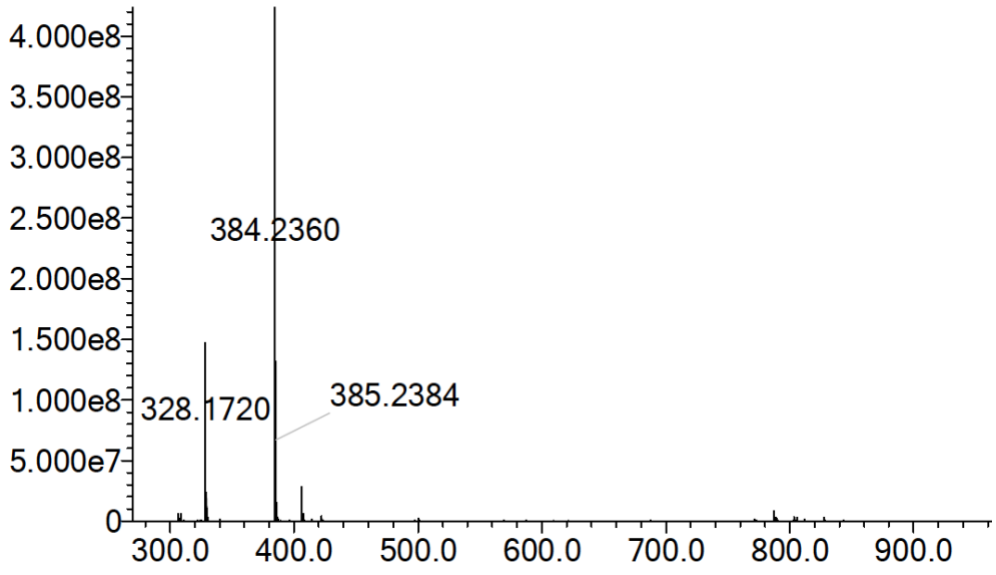

Figure 3. Mass spectrum of **1**. The line at m/z 384.2360 and 384.2384 correspond to the product. A line m/z ~406/407 corresponds to the sodium adduct. The line at 328.1720 is the result of fragmentation in the instrument wherein an isobutylene group (C_4H_8) from BOC is lost.

After confirming a successful synthesis of **1,** installation of the acetal is affected using EDC as a coupling agent. Upon extraction and chromatography, a 23% yield of **I** is obtained. Optimization has improved this yield.[12] The synthesis of the monomer, **I**, was confirmed by ^{1}H and ^{13}C NMR obtained in DMSO-*d*$_6$ using a similar approach (**Figures 4** and **5).**

A mass spectrum was obtained to verify the synthesis of the monomer (**Figure 6)**. The experimentally determined mass (M_{exp} = 513.3517 Da) matches the predicted mass (M_{pred} = 513.3507 Da) of the monomer, **I.**

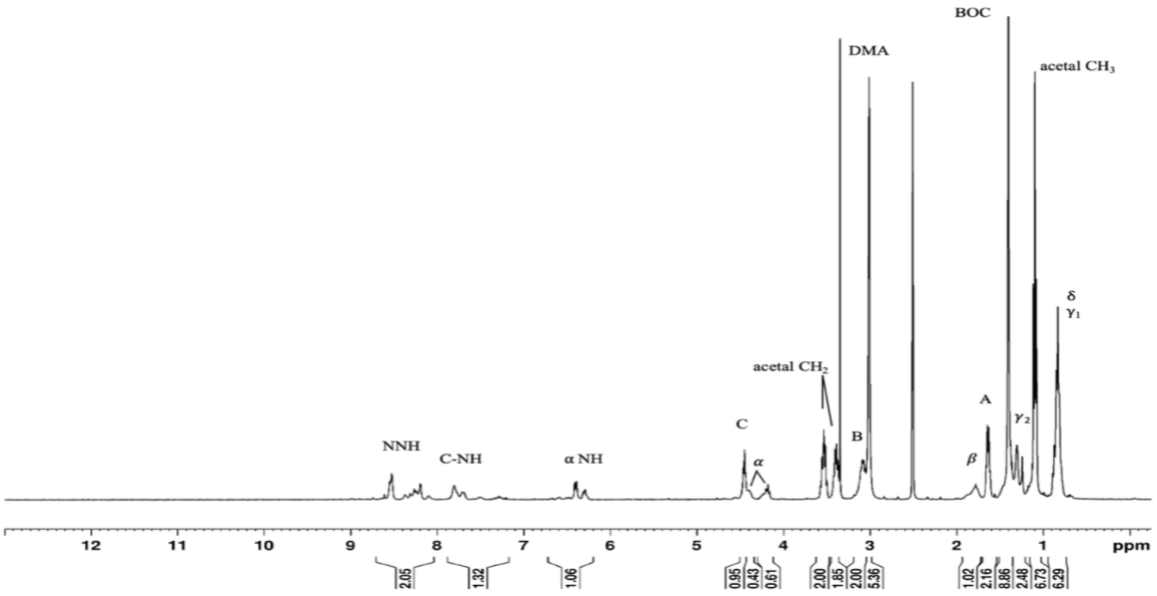

Figure 4. ^{1}H NMR spectrum of the monomer, **I**, in DMSO-*d*$_6$. Note the appearance of rotamers in the spectrum as evident by multiple resonances for a single proton(s).

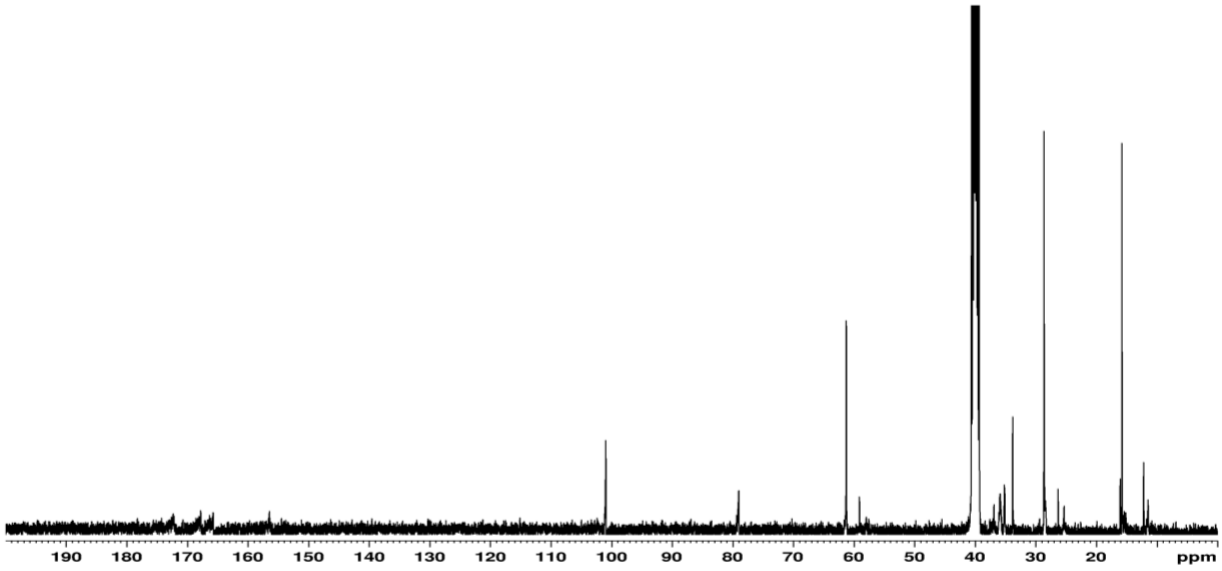

Figure 5. ^{13}C NMR spectrum of the monomer, **I**, in DMSO-*d*$_6$. The triazine portion of the spectrum between 175-165 ppm is broad due to the presence of rotamers.

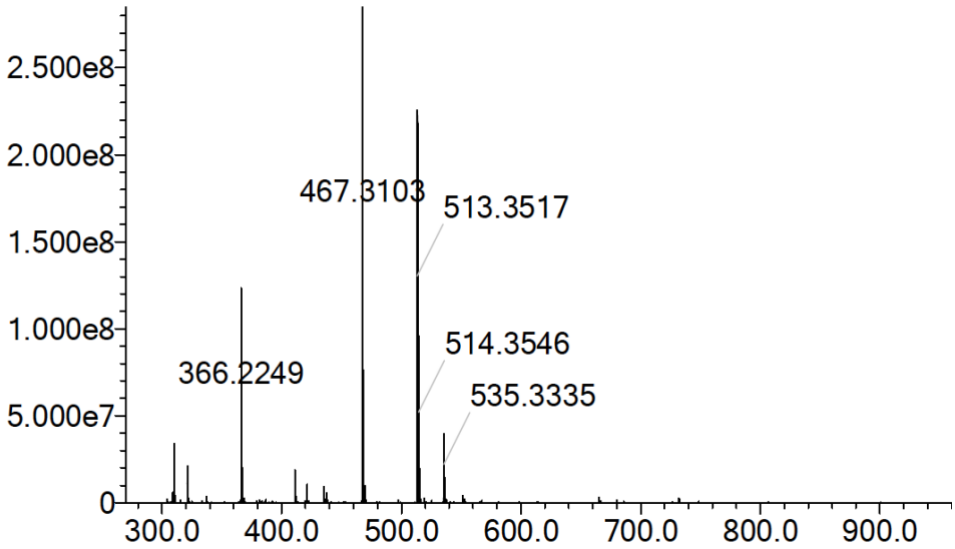

Figure 6. Mass spectrum of the monomer, **I**. The product is seen at m/z 413. A sodium adduct is visible at m/z 535. Fragmentation during the experiment gives rise to m/z 467 (loss of -OCH_2CH_3) and m/z 366 (loss of BOC).

Again, the ^{1}H NMR is most useful for verifying synthesis. The identifying acid peak at 12.4 ppm corresponding to the carboxylic acid that reacts is no longer present. Instead, there is a multitude of new peaks correlating to the acetal. The CH_2 groups in the acetal are present at 3.54 and 3.39 ppm. The terminal methyl groups of the acetal appear at 1.10 ppm. These peaks, along with the presence of A and B, validate the synthesis of the monomer, **I**. Like the acid **1**, the monomer, **I,** presents evidence of multiple conformations. The ^{13}C NMR is also consistent. The synthesis of the monomer is confirmed by the presence of a new peak at 100 ppm correlating to an electron-rich carbon, the acetal. The presence of the acetal resonance and evidence of multiple confirmations confirms the monomer.

Synthesis, Characterization, and Conformational Analysis of Macrocycle, ***I-I****.* Dimerization of **1** to yield the macrocycle proceeds quantitatively and does not require purification. Dissolution of the monomer in 1:1 mixtures of dichloromethane:trifluoroacetic acid yields macrocycles, but only upon slow evaporation of the solvent. The concentration of the monomer was 17.5 mg/mL, but macrocyclization has been shown to occur in concentrations between 5 mg/mL and 125 mg/mL. The synthesis of **I-**I was confirmed by ^{1}H and ^{13}C NMR spectroscopy.

The first indication of a successful synthesis is the simplicity of the ^{1}H NMR spectra of **I-I** compared to that of the monomer **I** and the acid intermediate, **1 (Figure 7)**. The terminal ethyl group resonances of the acetal are no longer present. New resonances appear including the resonance at 12.6 ppm corresponding to the NN<u>H</u> proton. The A proton moves from 4.5 ppm to 7.5 ppm.

The ^{13}C NMR is also consistent (**Figure 8)**. There is a loss of a peak at 100 ppm, the acetal. Additionally, a new resonance appears at 147 ppm and is representative of A (HC=N). A mass spectrum was obtained to verify the synthesis of the macrocycle (**Figure 9**). The experimentally determined mass (M_{exp} = 641.4232 Da) matches the predicted mass (M_{pred} = 641.4219 Da) of the macrocycle, **I-I.**

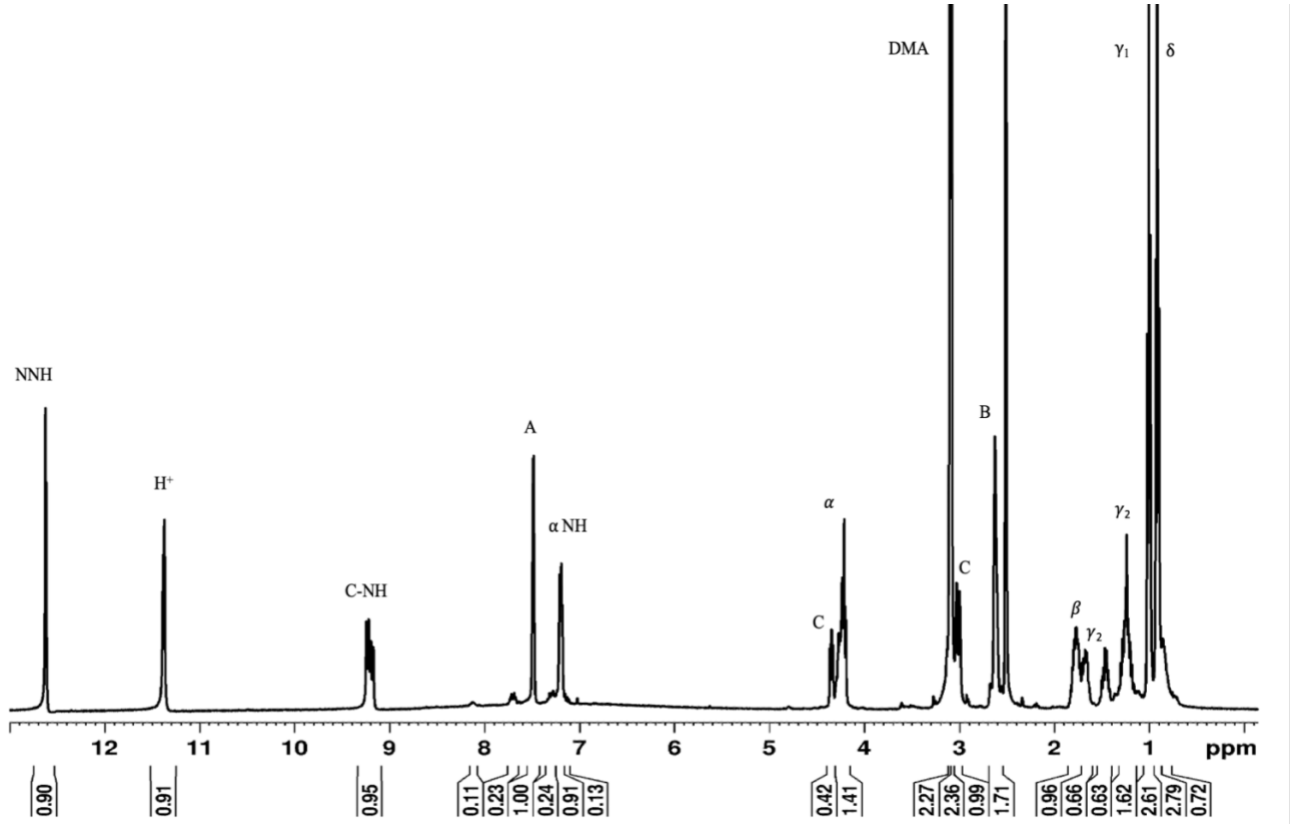

Figure 7. ^{1}H NMR spectrum of the macrocycle, **I-I**, in DMSO-d_6.

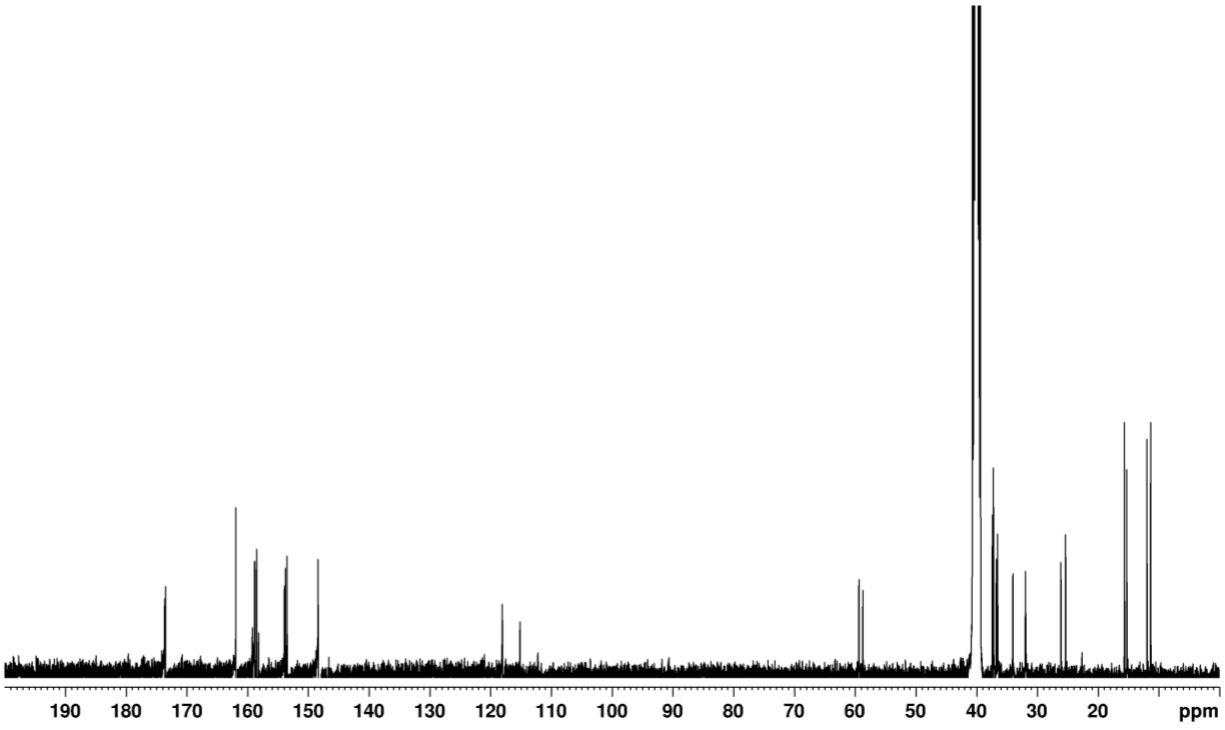

Figure 8. ^{13}C NMR spectrum of the macrocycle, **I-I**, in DMSO-*d*$_6$.

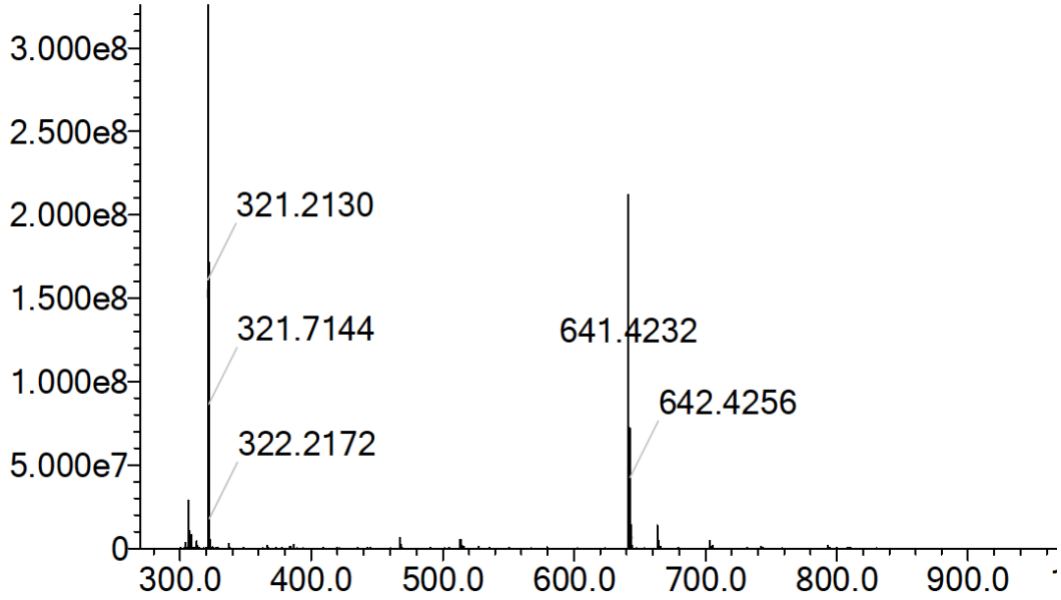

Figure 9. Mass spectrum of the macrocycle, **I-I**. The doubly charged macrocycle appears at m/z 321.

The spectra of **I-I** can be easily assigned using a COSY experiment which shows correlations between hydrogens on adjacent carbon atoms. That is, these hydrogens that are near each other and connected by one or two carbon atoms can "see" each other, a relationship called "coupled," as shown by a data point in the COSY spectra (**Figure 10)**. These coupling correlations allow quick and unambiguous proton assignment.

For example, based on the structure, α-NH should only be coupled to α. This belief is consistent with the COSY spectrum and shown with the blue lines. Once α is determined, it is possible to assign the other isoleucine peaks. The strong peak at 7.48 ppm is characteristic of the hydrazone, denoted by A. Based on the COSY spectrum, proton A has connectivity to protons B and C. All protons in the structure can be assigned in a similar manner.

Upon completion of the assignment, an interesting observation emerges. One-dimensional NMR spectroscopy provides evidence for two different macrocycles. While the simplicity of **I-I** is apparent, especially when compared to the monomer, most resonances appear twice in a common ratio of 60:40.

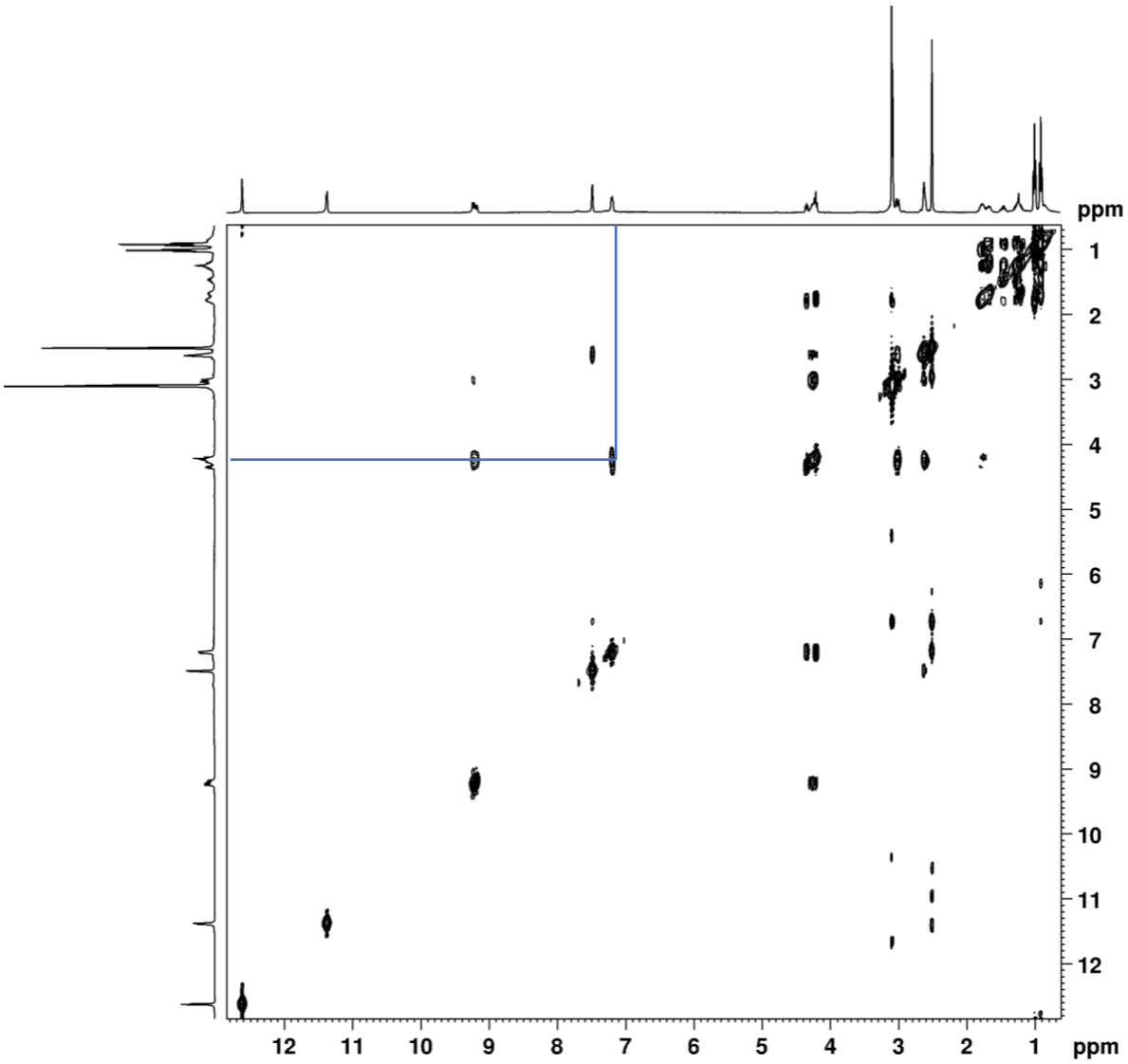

Figure 10. ^{1}H-^{1}H COSY spectrum of the macrocycle, **I-I**, in DMSO-*d*$_6$.

To explain why two isomeric products were obtained, variable temperature NMR spectra were recorded. When the ^{1}H NMR spectrum of the macrocycle, **I-I**, was taken at room temperature, -20 ^{o}C, -40 ^{o}C, and -60 ^{o}C in deuterated methanol, there was no evidence for the appearance of new conformations **(Figure 11).** All the spectra remain sharp, and the 60:40 ratio is preserved. Additional experiments at higher temperatures were performed. At 50 ^{o}C, the two isomers are still observed. At 60 ^{o}C in DMSO-*d*$_6$, the resonances for the two isomers coalesce (merge), indicating

that only one molecule is present that exists as two slowly interconverting isomers at room temperature (data not shown). The absolute structures of these isomers is currently unknown.

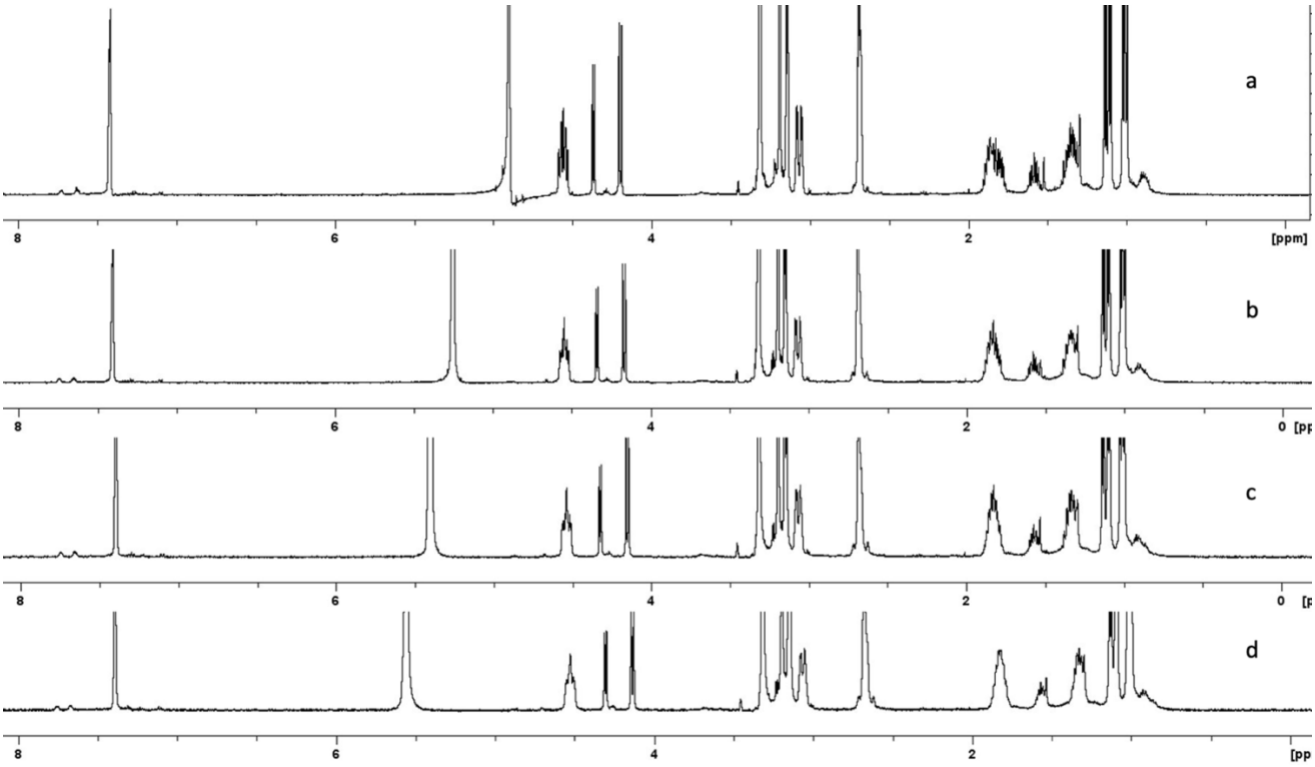

Figure 11. Low-temperature study for the macrocycle, **I-I**, in MeOD-d_4 a) at room temperature b) at -20 ^{o}C c) at -40 ^{o}C d) at -60 ^{o}C.

Probing the shape of the molecule. While it was determined that the macrocycle is symmetric, we still do not have evidence of the 3-D shape of the molecule in solution. Some clues can be discerned from the NMR spectra already recorded. There is a possibility that different isomers are observed in the NMR spectra of the macrocycle due to slow rotation around the triazine-N bond. Four rotational isomers are possible for triazine rings **(Figure 12).** Only one of these rotational isomers exists for the two **I-I** macrocycles in 60:40 ratios.

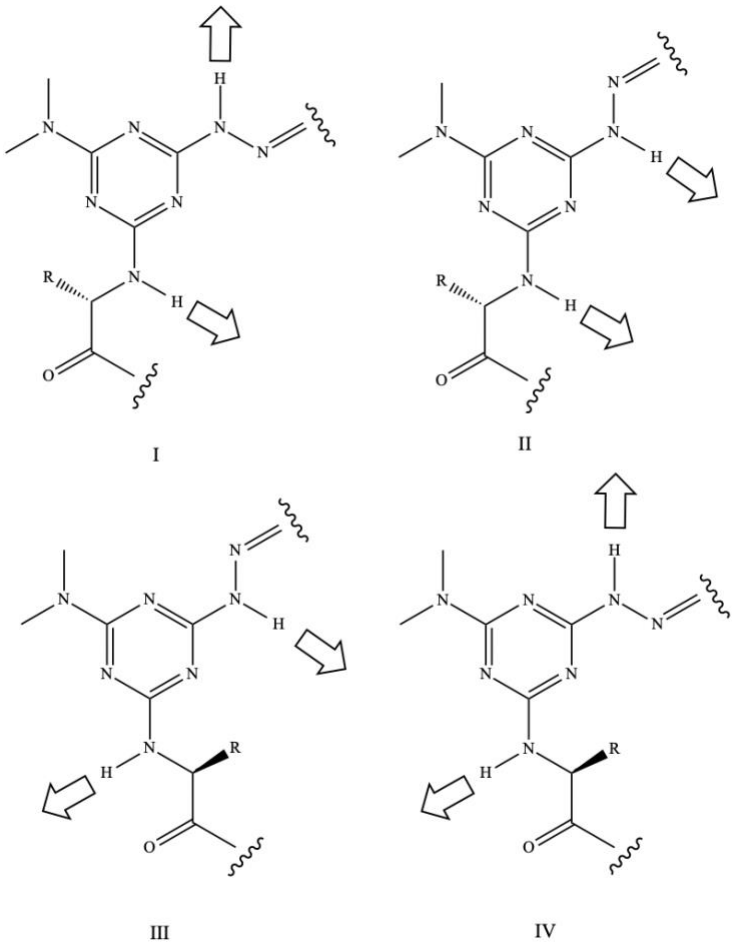

Figure 12. Four possible rotamers for triazines.

To probe shape, we look for "coupled" hydrogens that see each other through space (not through bonds). This 2D NMR experiment is called a rOesy **(Figure 13).** Using the rOesy experiments in DMSO, we find that the major species for both isomers (60:40) exists as rotamer I. This conformation is representative of a trans hydrazone, as NNH does not see H^+. It is also determined that α-NH can see H^+, as shown by the blue lines, meaning α-NH points towards the middle of the macrocycle. Other correlations observed are consistent with a *trans*-hydrazone (NNH sees A, green lines).

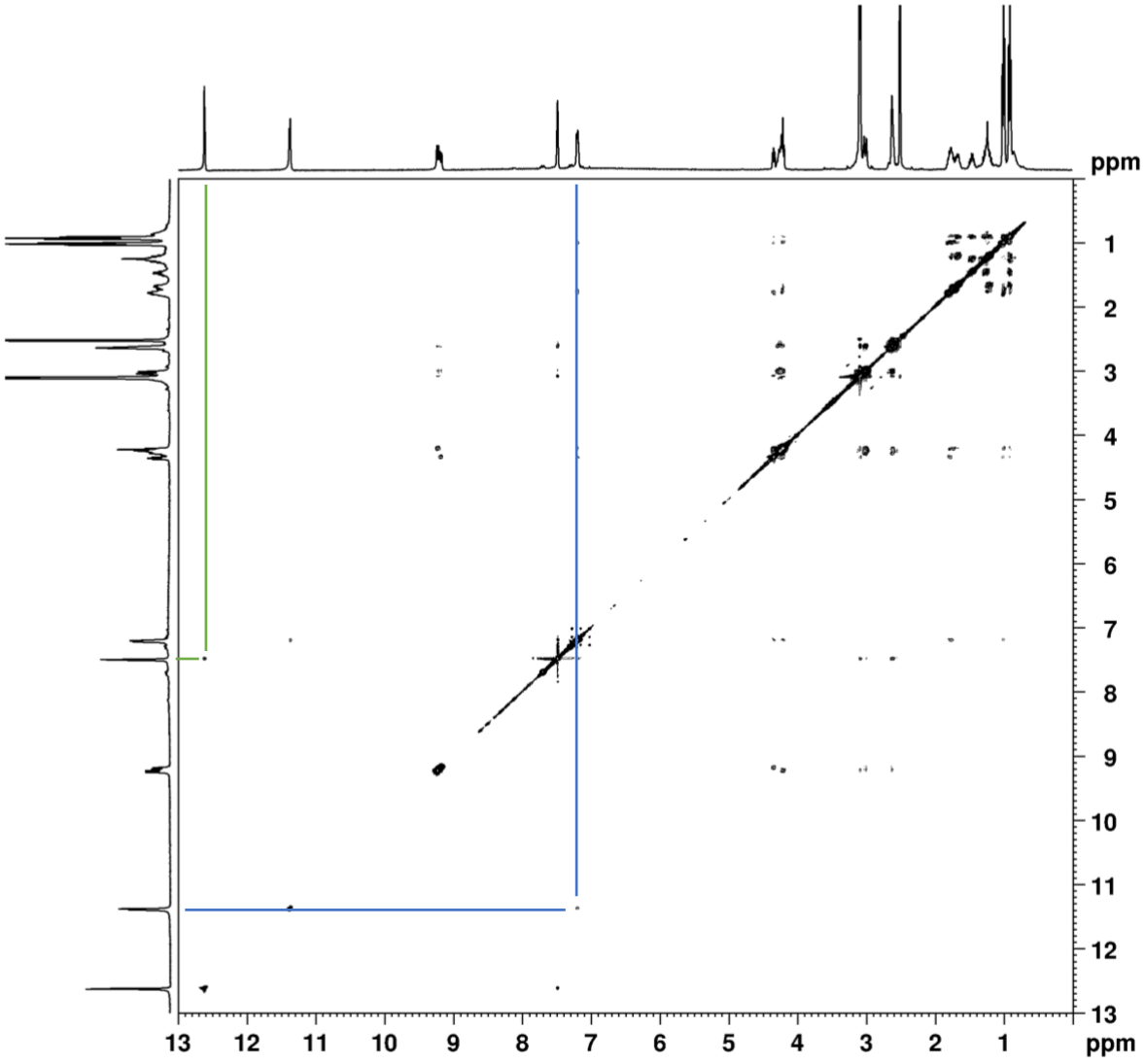

Figure 13. rOesy spectrum of the macrocycle, **I-I**, in DMSO-d_6.

The final evidence for shape (or lack thereof) comes with rOesy correlations that are missing. Other macrocycles have been shown to clearly fold in both solution and solid-state. The lack of a strong rOe between the DMA groups and the NNH or A suggests that the conformation of these isomers might be more extended. Additional work is needed.

CONCLUSION

Macrocycle **I-I** is available in three synthetic steps. Beginning with cyanuric chloride, three substitution reactions are undergone with BOC-hydrazine, isoleucine, and dimethylamine to give the acid intermediate, **1,** at an 8.6% yield. The acid undergoes an EDC coupling reaction to give the monomer, I, at a 23% yield. Spontaneous dimerization with the addition of trifluoroacetic acid gives the monomer **I-I.** Synthesis was confirmed by ^{1}H and ^{13}C NMR experiments in DMSO. Based on the simplicity of the ^{1}H NMR for the macrocycle, we have established that the macrocycle is highly symmetric and exists in two different shapes at room temperature that interconvert at higher temperatures. This hypothesis is supported by a variable temperature ^{1}H NMR study, which showed only one conformation for each isomer at low temperatures and their coalescence at high temperatures. Elements of the solution structure of **I-I** can be assigned in DMSO-d_6 based on a network of rOe. This study revealed two rotamers of the triazine ring in a 6:4 ratio. Both isomers have a *trans*-hydrazone and α-NH pointing towards the middle of the macrocycle seeing H^{+}, implicating rotamer **I**.

The successful synthesis of an isoleucine-containing macrocycle is promising for the future of drug design. An essential aspect of drug design is the ability to control the shape of the molecule. While the previous macrocycles synthesized containing glycine and *beta*-alanine were single symmetrical species that interconverted rapidly, isoleucine, a bulky *beta*-branched amino acid, adds steric bulk to the macrocycle, slowing down its ability to interconvert. Additionally, this macrocycle is the first in which persistent isomers are present. The inclusion of isoleucine in a macrocycle gives the ability to better control the shape of the macrocycle by introducing multiple isomers.

REFERENCES

1. Vinogradov, A. A.; Yin, Y.; Suga, H. Macrocyclic Peptides as Drug Candidates: Recent Progress and Remaining Challenges. *J. Am. Chem. Soc.* **2019**, *141* (10), 4167–4181. https://doi.org/10.1021/jacs.8b13178.

2. Giordanetto, F.; Kihlberg, J. Macrocyclic Drugs and Clinical Candidates: What Can Medicinal Chemists Learn from Their Properties? *J. Med. Chem.* **2014**, *57* (2), 278–295. https://doi.org/10.1021/jm400887j.

3. Dougherty, P. G.; Sahni, A.; Pei, D. Understanding Cell Penetration of Cyclic Peptides. Chem. Rev. 2019, 119 (17), 10241–10287. https://doi.org/10.1021/acs.chemrev.9b00008.

4. Naylor, M. R.; Ly, A. M.; Handford, M. J.; Ramos, D. P.; Pye, C. R.; Furukawa, A.; Klein, V. G.; Noland, R. P.; Edmondson, Q.; Turmon, A. C.; Hewitt, W. M.; Schwochert, J.; Townsend, C. E.; Kelly, C. N.; Blanco, M.-J.; Lokey, R. S. Lipophilic Permeability Efficiency Reconciles the Opposing Roles of Lipophilicity in Membrane Permeability and Aqueous Solubility. *J. Med. Chem.* **2018**, *61* (24), 11169–11182. https://doi.org/10.1021/acs.jmedchem.8b01259.

5. Benet, L. Z.; Hosey, C. M.; Ursu, O.; Oprea, T. I. BDDCS, the Rule of 5 and Drugability. *Adv. Drug Deliv. Rev.* **2016**, *101*, 89–98. https://doi.org/10.1016/j.addr.2016.05.007.

6. Lipinski, C. A.; Lombardo, F.; Dominy, B. W.; Feeney, P. J. Experimental and Computational Approaches to Estimate Solubility and Permeability in Drug Discovery and Development Settings. *Adv. Drug Deliv. Rev.* **2012**, *64*, 4–17. https://doi.org/10.1016/j.addr.2012.09.019.

7. DeGoey, D. A.; Chen, H.-J.; Cox, P. B.; Wendt, M. D. Beyond the Rule of 5: Lessons Learned from AbbVie's Drugs and Compound Collection: Miniperspective. *J. Med. Chem.* **2018**, *61* (7), 2636–2651. https://doi.org/10.1021/acs.jmedchem.7b00717.

8. Kamenik, A. S.; Lessel, U.; Fuchs, J. E.; Fox, T.; Liedl, K. R. Peptidic Macrocycles - Conformational Sampling and Thermodynamic Characterization. *J. Chem. Inf. Model.* **2018**, *58* (5), 982–992. https://doi.org/10.1021/acs.jcim.8b00097.

9. Sharma, V. R.; Mehmood, A.; Janesko, B. G.; Simanek, E. E. Efficient Syntheses of Macrocycles Ranging from 22–28 Atoms through Spontaneous Dimerization to Yield Bis-Hydrazones. *RSC Adv.* **2020**, *10* (6), 3217–3220. https://doi.org/10.1039/c9ra08056b.

10. Cummings, A. E.; Miao, J.; Slough, D. P.; McHugh, S. M.; Kritzer, J. A.; Lin, Y.-S. B-Branched Amino Acids Stabilize Specific Conformations of Cyclic Hexapeptides. Biophys. J. 2019, 116 (3), 433–444. https://doi.org/10.1016/j.bpj.2018.12.015.

11. Chatterjee, J.; Gilon, C.; Hoffman, A.; Kessler, H. N-Methylation of Peptides: A New Perspective in Medicinal Chemistry. Acc. Chem. Res. 2008, 41 (10), 1331–1342. https://doi.org/10.1021/ar8000603.

12. Menke, A.; Gloor, C.; Claton, L. Simanek, E.; Structural Tolerance of b-Branched Amino Acids within 24-atom Macrocycles. Manuscript in progress.

13. Bentz, W. E., Colebrook, L. D., Fehlner, J. R., & Rosowsky, A. (1970). Hindered rotation about C–N bonds: equilibration of diastereomeric rotational isomers. *J. Chem. Soc. D*, *0*(16), 974–974. https://doi.org/10.1039/c29700000974